Technical Challenges and Progress in GaN Crystal Growth and Processing

Sumitomo Chemical Co., Ltd.
ICT & Mobility Solutions Research Laboratory
Seiji SARAYAMA
Takashi SATO

GaN crystals are difficult to grow and process because many defects occur during crystal growth, and damage layers form easily and are difficult to remove during crystal processing. This study addresses the challenges associated with growing and processing GaN crystals, which are caused by their characteristic and properties. Inversion domains, crystal defects generated during crystal growth, are resolved by combining vapor and liquid phase growth. Moreover, damage layers formed during fabrication is removed by chemical mechanical polishing.

Introduction

Gallium nitride (GaN) is a direct-bandgap semiconductor material with a bandgap of 3.4 eV. Since the 1990s, blue light-emitting diodes (LEDs), white LEDs, and blue–violet laser diodes (LDs) have been commercialized, and research and development continues with the goal of applying GaN to power devices.

In this paper, we describe the challenges in crystal growth arising from the unique characteristics of GaN crystals compared with other semiconductor crystals, based on the history of the research and development of crystal-growth technology to date. We also discuss the issues facing power-device applications, which are anticipated to see future advancement, along with the new solutions being developed. Furthermore, crystal-processing technology, which converts bulk GaN crystals obtained through crystal growth into wafers, is as critical as crystal growth itself. GaN crystal processing is challenging, and the second half of this paper examines the reasons for these challenges, along with the final finishing process, which is one of the most essential processing steps.

GaN crystal growth

1. Characteristics and growth methods of GaN crystals

(1) Characteristics of GaN crystals

The semiconductor crystals germanium (Ge), silicon (Si), gallium arsenide (GaAs), and indium phosphide (InP), which have long been used in devices, have melting points ranging from approximately 930 to 1420 °C, as indicated in **Table 1**. The single-element semiconductors Ge and Si have extremely low vapor

Table 1 Melting point and vapor pressure of semiconductor crystal materials[1), 2), 3)]

Semiconductor crystal material	Melting point (°C)	Vapor pressure (atm)	Vapor element
Ge	938	10^{-9}	Ge
Si	1,414	10^{-6}	Si
GaAs	1,238	1	As
InP	1,067	3.85	P
GaN	2,200	6×10^{4}	N

pressures near their melting points, at 10^{-9} and 10^{-6} atm, respectively. The vapor pressures of the group V elements found in the compound semiconductors GaAs and InP are 1.0 and 3.85 atm, respectively, which are higher than those of single-element semiconductors but remain at the level of only a few atmospheres. The fact that these vapor pressures can be artificially controlled enables melt growth when implementing crystal growth. Consequently, ingots solidified from the melt can be grown as single crystals, producing large-diameter, long ingots similar to those of Si (e.g., with a diameter ≥ φ300 mm and length of several meters).

In contrast, GaN struggles to exist as a melt as a result of the high nitrogen dissociation pressure[4], and its existence has been confirmed only at 2,220 °C and 6×10^4 atm (6 GPa)[3]. Producing large crystals at such temperatures and pressures is extremely challenging, and GaN crystal ingots with a practical size (i.e., at least one inch in size) have not yet been obtained by solidification from the melt.

Therefore, heteroepitaxial growth on sapphire substrates is frequently employed (the term "epitaxial" originates from the Greek words *epi* ("on –") and *taxy* ("aligned"), which means the crystals grow upward with aligned crystal axes). GaN crystal structures include wurtzite-type hexagonal and zinc-blend-type cubic structures, with the former being the most stable phase and the latter being a metastable phase. Sapphire, which is an aluminum oxide (Al_2O_3) single crystal, also has a hexagonal crystal structure and remains stable even at temperatures above 1,000 °C under various GaN crystal growth processes, as described below. Therefore, sapphire is used as a substrate for heteroepitaxial GaN growth despite its substantial differences from GaN in terms of the thermal expansion coefficient (25%) and lattice constant (14%)[5].

(2) Various GaN crystal growth methods

Table 2 lists the main GaN crystal growth methods, which can be broadly categorized into vapor-phase growth and liquid-phase growth.

The main vapor-phase growth methods are metal-organic vapor-phase epitaxy (MOVPE), hydride vapor-phase epitaxy (HVPE), and vapor-phase synthesis. MOVPE, which is also called metal-organic chemical vapor deposition (MOCVD), is a method for the epitaxial growth of GaN crystals on a substrate using organic metals as the Group III source and ammonia gas (NH_3) as the Group V source. HVPE is a method for the epitaxial growth of GaN crystals on a substrate using gallium chloride as the Group III source and ammonia gas (NH_3) as the Group V source. Vapor-phase synthesis involves growing GaN crystals by supplying heated metallic gallium as the Group III source and using nitrogen gas (N_2) or ammonia gas (NH_3) as the Group V source. MOVPE has a growth rate of several micrometers per hour, whereas HVPE is faster, reaching several hundred micrometers per hour. MOVPE can use not only Ga, but also organic metals such as Al and In to grow AlN, InN, and their alloys. Because of these differing characteristics, MOVPE is often employed to grow thin films for device fabrication, whereas HVPE

Table 2 Various methods of GaN crystal Growth

Method			Characteristic
Vapor phase growth	MOVPE (Metal organic vapor phase epitaxy)		Thin film GaN crystals grown using a metal organic source and ammonia gas on a substrate
	HVPE (Hydride vapor phase epitaxy)		Thick film GaN crystals grown using a metal chloride source and ammonia gas on a substrate
	Vapor phase composition[6]		GaN crystals grown using metal Ga vapor and NH_3, N_2 at ~1,200 °C
Liquid phase growth	Melt growth[3]		GaN crystals grown by slow cooling using N_2 at high temperatures and pressures (6GPa, ~2,200 °C)
	Solution growth	High pressure solution growth method[7]	GaN crystals grown by supersaturation control in metal Ga with dissolved N_2 at high temperatures (1600 °C) and pressures (1–2GPa)
		Flux method[8]	GaN crystals grown using a mixed melt consisting of metal Ga and alkali metal (mainly Na) with N_2 at a temperature 800-900 °C and a pressure of <10 MPa
		Ammono-thermal method[9]	GaN crystals grown using poly crystals dissolved and regrown in supercritical or subcritical NH_3

is typically used to grow thick films to produce GaN substrates. Vapor-phase synthesis uses Ga vapor as the Group III source, which simplifies the reaction system compared to other methods. However, the method has not been widely adopted because of concerns about the crystal quality and growth rate, and only MOVPE and HVPE are used practically.

Liquid-phase growth methods include melt growth and solution growth. However, as noted above, melt growth is difficult at practical temperatures and pressures. Thus, solution growth is more commonly used. Solution-growth methods include the high-pressure solution method, flux method, and ammonothermal method. The high-pressure solution method grows GaN crystals by dissolving nitrogen from ultra-high-pressure (10,000–20,000 atm) nitrogen gas (N_2) into a high-temperature (1,600 °C) Ga melt. The flux method melts alkali metals and metallic gallium at approximately 800–900 °C and dissolves nitrogen from nitrogen gas at a level of tens of atmospheres to grow GaN crystals. The ammonothermal method involves dissolving polycrystalline GaN as a raw material in supercritical or subcritical ammonia (thousands of atmospheres, several hundred degrees Celsius) and recrystallizing it.

Among these crystal growth methods, HVPE is currently the only one in practical use for producing GaN substrates, although ammonothermal and flux method-based GaN substrates are starting to become commercially available. In practical terms, vapor-phase growth is the leading method, followed by liquid-phase growth. Research and development continues on the use of HVPE as well as ammonothermal and flux methods to further improve the crystal quality and enlarge the substrate area.

2. History of GaN crystal growth: Realization of GaN substrates

As mentioned above, heteroepitaxial growth on sapphire substrates is widely used for GaN crystal growth. **Fig. 1** illustrates the major developments in this crystal-growth technology. In **Fig. 1**, the horizontal axis represents the time period, and the vertical axis represents the distinction between thin-film growth by MOVPE and thick-film growth by HVPE. There is generally no clear boundary between thin and thick films, but we will use a film thickness of approximately 10 μm as the dividing line here. The numbers in circles in the figure correspond to the cited reference numbers.

A paper published in 1969 reported that GaN crystals with a thickness of 0.25 mm (250 μm) were grown on sapphire substrates using HVPE, and a direct transition with a bandgap, E_g, of approximately 3.39 eV was observed from optical absorption[10]. Subsequently, a paper published in 1971 reported the fabrication of a blue LED with a metal–insulator–semiconductor (MIS) structure, which included a GaNi-n layer with a thickness of 22.4 μm grown using HVPE. No improvement in GaN crystal quality was subsequently observed, and the research and development of crystal-growth technology reached a plateau[11].

This situation was overcome by several technological breakthroughs in the late 1980s and 1990s, including high-quality crystal-growth technology that used low-temperature buffer layers[12), 13)] and p-type dopant doping and activation technology[14), 15)]. The application of these

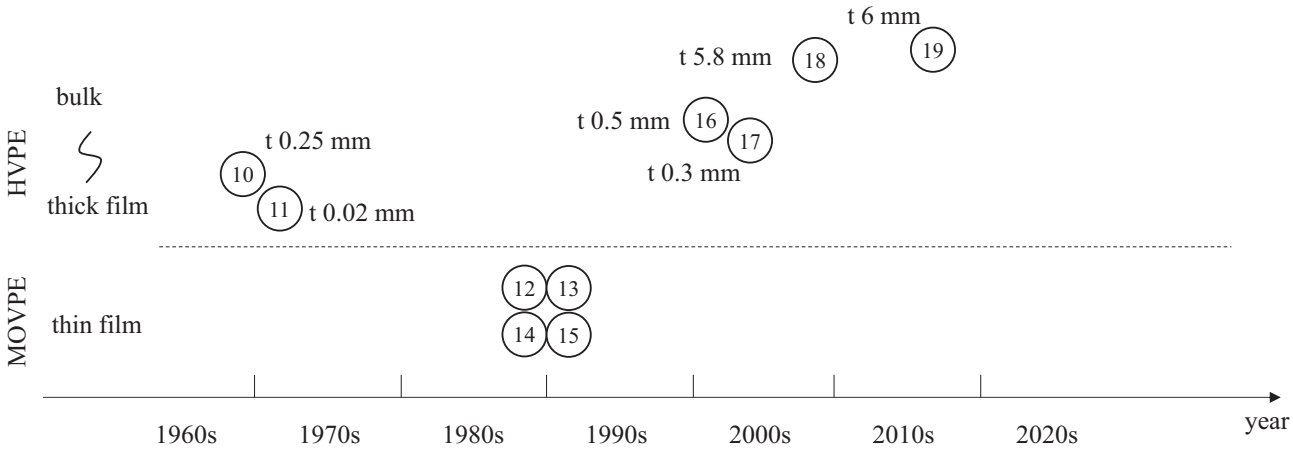

Fig. 1 Transition of GaN crystal growth
(*t*: GaN crystal thickness)

technologies led to the practical application of blue LEDs, white LEDs, and blue–violet LDs (low-power products with optical outputs of a few microwatts). All of these were grown on sapphire substrates using MOVPE, and high-density threading dislocations ($\geq 10^8$ cm^{-2}) existed in the GaN crystals as a result of the abovementioned differences in the lattice constants and thermal expansion coefficients of sapphire and GaN.

Subsequently, in the 2000s, thick-film growth and heterosubstrate removal and separation techniques were developed using HVPE, which enabled the fabrication of GaN substrates, and led to the announcement of several free-standing GaN substrates. One of these techniques was the dislocation elimination by epitaxial growth with inverse pyramidal pits (DEEP) method, which was reported in 2001. This method forms inverted hexagonal pyramidal pits (depressions) and concentrates dislocations at their centers, which results in the formation of low-threading dislocation density (TDD) domains outside the centers. The TDD of these domains was 2×10^5 cm^{-2}, which represents a three-orders-of-magnitude reduction compared with the value for conventional heteroepitaxial growth, and free-standing GaN substrates with a thickness of 500 μm were obtained[16]. Another technique was the void-assisted separation (VAS) method, which was reported in 2003. This involves thermally separating thick GaN crystals via a TiN layer[17]. The VAS method was shown to produce GaN substrates with a uniform TDD of 5×10^6 cm^{-2} across the entire plane.

The realization of GaN substrates with reduced TDD has led to a higher output power and wider wavelength domain for blue–violet LDs, enabling their practical use as light sources for high-speed optical disc writing and displays. The substrates for these LDs typically have diameters of approximately 2 inches (50.8 mm). Power-electronic device applications, which are expected to contribute to energy conservation in the future, require not only larger diameters but also cost reductions and improvements in the crystal quality, such as a reduced TDD.

3. Challenges in producing GaN substrates for power-electronic device applications

GaN crystals are typically grown using epitaxial growth along the <0001> axis (+c-axis), perpendicular to the c-plane, to increase the crystal thickness. During this process, semi-polarity planes such as the {10$\bar{1}$1} and {10$\bar{1}$2} planes appear at the crystal edges as growth planes (facets) other than the c-plane. These semi-polarity planes are obliquely angled relative to the c-axis (e.g., the {10$\bar{1}$1 } plane is at approximately 62° relative to the c-plane). Thus, the area of the c-plane decreases as the film thickness increases. Increasing the crystal thickness increases the number of substrates that can be obtained from a single crystal, which leads to lower costs. However, because the area decreases, there is a trade-off between a larger diameter and lower cost.

A paper published in 2009 reported that GaN bulk crystals could be grown via HVPE to increase the film thickness[18], achieving a crystal thickness of 5.8 mm along the c-axis. We sell GaN substrates produced using the abovementioned VAS method, and by fine-tuning the growth parameters for this technique, we have obtained GaN crystals with a thickness of 6 mm along the c-axis[19].

Increasing the crystal thickness in the +c-axis direction using HVPE may result in the appearance of inversion domains (IDs) with partially inverted polarity (domains in which portions of the N-polarity plane are exposed relative to the Ga-polarity plane on the main plane)[19]. In these IDs, pits develop as a result of differences in the growth rates of the N-polarity plane (–c plane) and Ga-polarity plane (+c plane), and high impurity concentrations form around the IDs. These pits and high impurity concentration domains range in size from micrometers to millimeters, and device fabrication employing these areas can result in unstable device characteristics and current leakage.

Fig. 2 illustrates the results of chemical mechanical polishing (CMP) on a domain where IDs have formed and +c planes and -c planes coexist, followed by shape evaluation using the coherence scanning interferometry (CSI) method. A scanning white light interferometer was utilized for assessment via the CSI method. The front side (+c plane) is displayed in the left column, and the back side (–c plane) is shown in the right column. The top rows (**Figs. 2(a)** and **(b)**) present differential plane images, and the middle rows (**Figs. 2(c)** and **(d)**) show cross-sectional profiles along the dashed line in the differential plane images. The bottom row (**Fig. 2(e)**) shows a schematic cross-sectional diagram based on these evaluations. Because the material removal rate (MRR) attained by CMP was higher on the –c plane than on the +c plane, unevenness arose due to material-removal differences between the +c and –c planes. **Figs. 2(a)** and **(c)** show that most of the front plane consisted of the +c plane, with domains exposing the –c plane

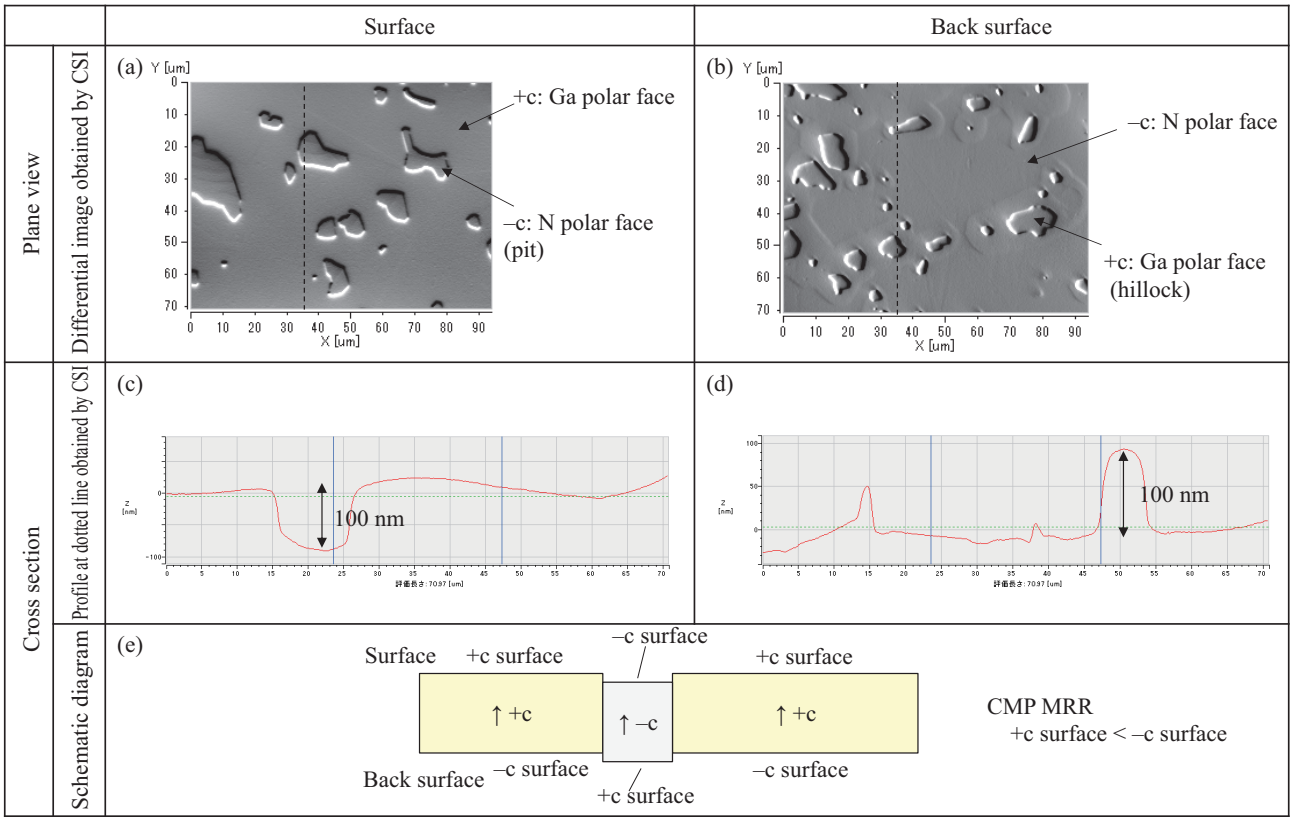

Fig. 2 Surface and back surface of the GaN crystal after processing (CMP)
(CSI: coherence scanning interferometry)

of the ID appearing as pits. In contrast, **Figs. 2(b)** and **(d)** reveal that most of the back plane was the –c plane, with domains where the +c plane of the ID was exposed appearing as hillock-like formations. The left and right columns in **Figs. 2(a)–(d)** do not show the same domains on the front and back planes. However, as described later, when an N-polarity plane exists on a Ga-polarity plane, the ID persists and grows in a direction that penetrates the crystal. We inferred the result shown in **Fig. 2(e)** based on these observations.

These IDs become problematic when enlarging the film area and thickness, and research has shown that optimizing the growth conditions of the HVPE method can mitigate this issue[19]. In the following section, we present a new method for eliminating IDs that combines the HVPE and flux methods.

4. Eliminating ID by combining HVPE and flux methods

Among the various crystal-growth techniques discussed in Section 1, we have expertise in the HVPE and sodium-based flux methods. This section presents the ID elimination results achieved by integrating these methods.

Fig. 3 shows a photograph and cross-sectional schematic of a GaN substrate with IDs grown via the HVPE method. **Fig. 3(a)** is a top-view photograph of the entire GaN substrate, with IDs appearing as pits in the black scattered regions. **Figs. 3(b)** and **(c)** show the top-view and cross-sectional SEM images of these pits, respectively. These images demonstrate that pits were distributed across the whole GaN substrate, with sizes ranging from tens to hundreds of micrometers. The pits had the form of inverted polygonal pyramids (hexagonal or dodecagonal pyramids), with the apex of a pyramid corresponding to the –c plane, which was an N-polarity plane (**Fig. 3(d)**). During HVPE crystal growth, the IDs persist. Thus, the pits are not eliminated. In contrast to HVPE, the Na flux method enables the growth of a Ga-polarity plane on an inverted N-polarity plane.

Fig. 4 presents a cross-sectional fluorescence microscopy image of a layered structure formed by planarizing an HVPE crystal with IDs and subsequently growing a GaN crystal using the Na flux method. The lower portion shows the HVPE crystal, with its Ga-polarity main plane appearing yellow, whereas the IDs and surrounding high-impurity-concentration domains appear brown. This cross-section shows two IDs;

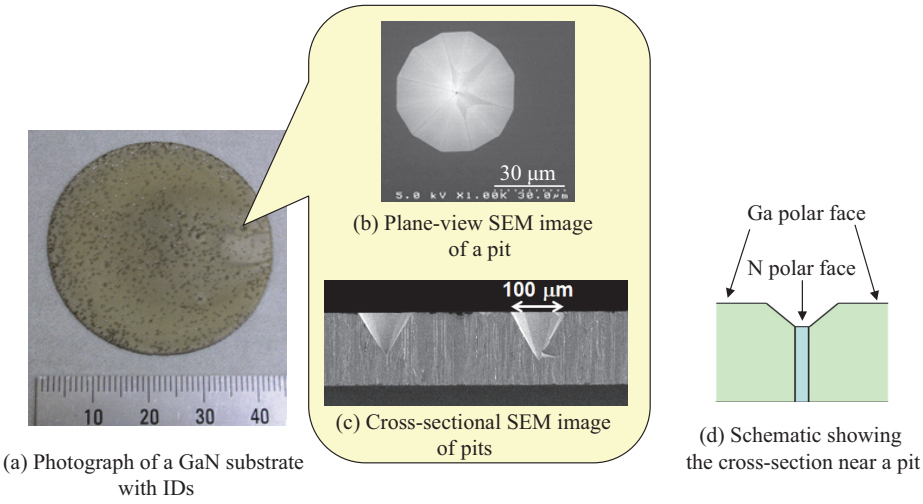

Fig. 3 Photograph showing a GaN substrate with inversion domains (IDs). Plane view and cross sectional SEM images

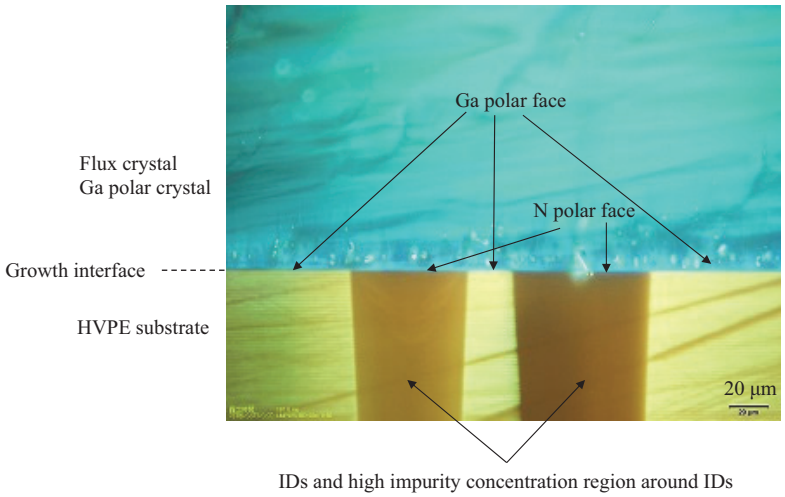

Fig. 4 Cross-sectional fluorescence microscopy image of an GaN crystal with IDs (flux crystal on a HVPE substrate)

however, the plane of the Na flux crystal grown above them is entirely a light-blue Ga-polarity plane (on non-polarity planes, Na flux crystal growth produces high-impurity-concentration domains, resulting in dark fluorescence rather than light blue). Furthermore, pits originating from the HVPE crystal IDs do not reappear during growth. Small white domains scattered on the flux crystal side of the growth interface (the boundary between the HVPE and Na flux crystals) represent Na-containing inclusions. The presence of these inclusions is believed to enable Ga-polarity crystal growth even on the IDs.

Fig. 5 shows a cross-sectional fluorescence microscope image of a GaN crystal grown by the Na flux method on an HVPE crystal with a pit on an ID. Pits associated with inverted polarity are present in the HVPE crystal. As shown in **Fig. 3**, these pits have an inverted polygonal pyramid shape, and **Fig. 5** shows a cross-section of this pyramid. Na flux crystals have grown directly above these pits, and the dark fluorescence indicates a high impurity concentration. Above this, Na flux crystals have grown on the Ga-polarity plane, showing light-blue to light-yellow fluorescence. **Fig. 5(b)** indicates that the domain grown on the non-polarity face of the Na flux crystal (dark fluorescence) diminishes above the growth interface. This suggests that the Na flux growth is faster on Ga-polarity planes than on semi-polarity planes, implying that IDs can be eliminated by the overgrowth of Ga-polarity planes over semi-polarity planes.

As discussed, Na flux growth enables Ga polarity plane growth across the entire plane regardless of the presence of IDs and pits, allowing the disadvantages of HVPE IDs to be resolved through combination with the Na flux method.

Fig. 6 displays TDD evaluation results for a Ga-

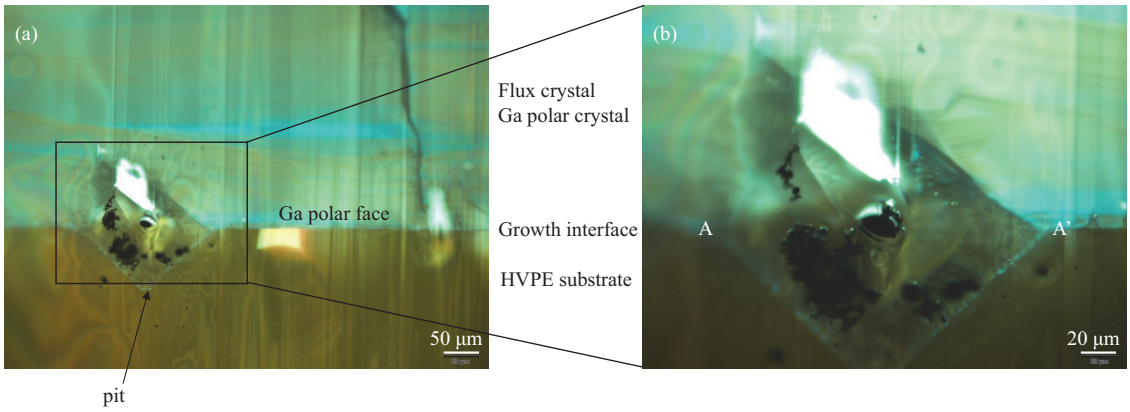

Fig. 5 Cross-sectional florescence microscopy images of a GaN crystal with an ID and a pit (flux crystal on a HVPE substrate)

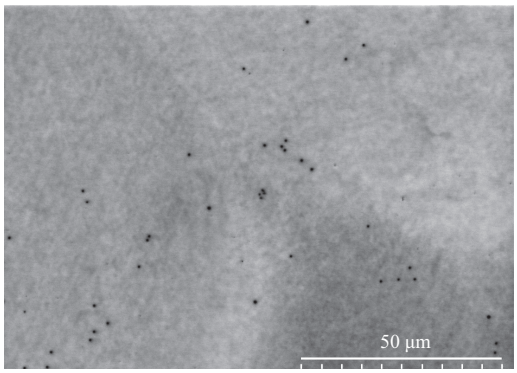

(a) Plane view CL (Cathode Luminescence) image
DSD (Dark Spot Density): 3.8 × 10^5 cm^{-2}
(DSs: 46) / (area size: 127 μm × 94 μm)

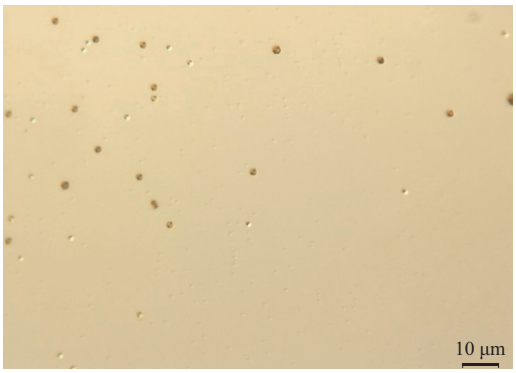

(b) Optical microscope (differential interference) image of EP (Etch Pit)
EPD (Etch Pit Density): 2.3 × 10^5 cm^{-2}
(EPs: 35) / (area size: 141 μm × 107 μm)

Fig. 6 Threading dislocation density (TDD) evaluation of the +c plane surface of the flux crystal (flux crystal on a HVPE substrate with an ID)

polarity plane grown via Na flux on an HVPE crystal with IDs. The TDD evaluation was conducted using cathode luminescence (CL) and etch pit (EP) techniques. **Fig. 6(a)** shows a CL image, and **Fig. 6(b)** shows a differential interference contrast image after EP formation. In the CL image, dislocations appear non-luminescent, with threading dislocations penetrating the +c plane visible as dark spots. The TDD could be calculated from the observed area size and number of dark spots. In **Fig. 6(a)**, the TDD derived from the dark-spot density is 3.8 × 10^5 cm^{-2}. Additionally, crystal dislocations, which are crystal defects that exist in single crystals, etch faster than dislocation-free domains and can be revealed using an etchant that is appropriate for the crystal material. For GaN crystals, etching with a high-temperature molten-alkali solution (potassium hydroxide (KOH) + sodium hydroxide (NaOH)) makes the dislocations visible, and dislocations that penetrate the etched surface become EPs. As in the CL image, the TDD calculated from the EP density was based on the number of pits and observed area. **Fig. 6(b)** shows a TDD of 2.3 × 10^5 cm^{-2} derived from EPs. The TDD values derived from both CL and EPs were in the low 10^5 cm^{-2} range, or roughly one order of magnitude lower than the TDD of 10^6 cm^{-2} for substrates fabricated using VAS with GaN crystals grown using HVPE.

As part of the efforts to scale up the wafer diameter, a 4-inch φ GaN crystal was grown via flux on an HVPE substrate with an ID (**Fig. 7**). A full Ga-polarity GaN crystal was obtained without cracks or breaks.

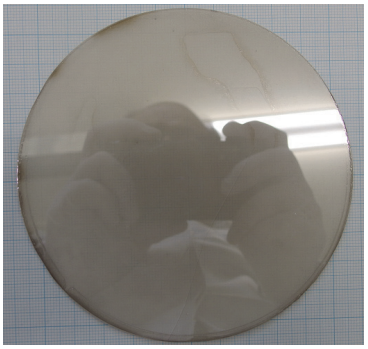

Fig. 7 ϕ 4 in (~101.6 mm) +c plane surface of a flux crystal on a HVPE substrate with IDs

GaN substrate processing

For semiconductor device fabrication, the ingot or bulk crystal must be shaped into wafers, as outlined in the previous section. As noted in Section 1 on "GaN crystal growth," large ingots can be grown by the melt growth of Si and GaAs, whereas GaN is grown as bulk crystals several millimeters thick, with substantially different shapes. Consequently, crystal processing techniques[20] developed for Si and GaAs cannot be directly applied, and three types of factors contribute to the difficulty of processing GaN crystal substrates[21].

(a) Physical property factors: Mechanical and chemical factors
(b) Crystal growth factor: Heteroepitaxial growth factors
(c) Crystal structure and crystal plane factors

The details of each of these factors are provided in Reference 21. In this study, we focused on CMP, which is the final finishing step in substrate processing.

1. Challenges with CMP of GaN crystals

To fabricate devices on GaN substrates, MOVPE is typically employed for the epitaxial growth of GaN-based thin films (GaN, InN, AlN, and their alloys) on a stable Ga-polarity plane. Thus, achieving a surface suitable for epitaxial growth is critical in the final stage of GaN substrate processing. In a strict sense, the surface quality varies with the MOVPE equipment and growth conditions. However, as a common denominator (a necessary condition required regardless of the MOVPE equipment and growth conditions used), an essential factor is removing the damaged layer created during crystal processing (i.e., the layer where the single crystal is mechanically damaged by crystal processing, causing the single crystal to become distorted and develop crystal defects, as described below). If this damaged layer remains, defects propagate vertically from this layer during epitaxial growth or device fabrication, causing current leakage and performance degradation of the device.

Generally, mechanical processes such as slicing, grinding, and polishing on a single crystal material create a damaged layer near the single crystal surface, but its depth is non-uniform. The damage is the greatest at the surface and decreases with depth. One study suggested that this damaged layer consists of an amorphous surface layer, followed by polycrystalline, mosaic, cracked, and distorted layers, with an underlying defect-free crystalline domain[22]. **Fig. 8** shows a cross-sectional transmission electron microscopy (TEM) image of the Ga-polarity plane of a Na flux-grown GaN crystal after diamond abrasive polishing. Disorders in the crystal lattice extend several hundred nanometers from the surface, with greater disorder near the surface. This indicates that amorphous, polycrystalline, mosaic, cracked, and distorted layers exist after GaN crystal processing, similar to those in other crystalline materials.

The difficulty of removing damaged layers in GaN crystals is attributed to the previously mentioned "(a) Physical property factors: Mechanical and chemical factors." **Fig. 9** compares the mechanical and chemical properties of GaN with those of Si and GaAs[21] in the form of a radar chart of Si and GaAs that plots the hardness, brittleness, and chemical stability values, with normalized values of 10 for GaN. The hardness is the Vickers hardness. The brittleness is the inverse of

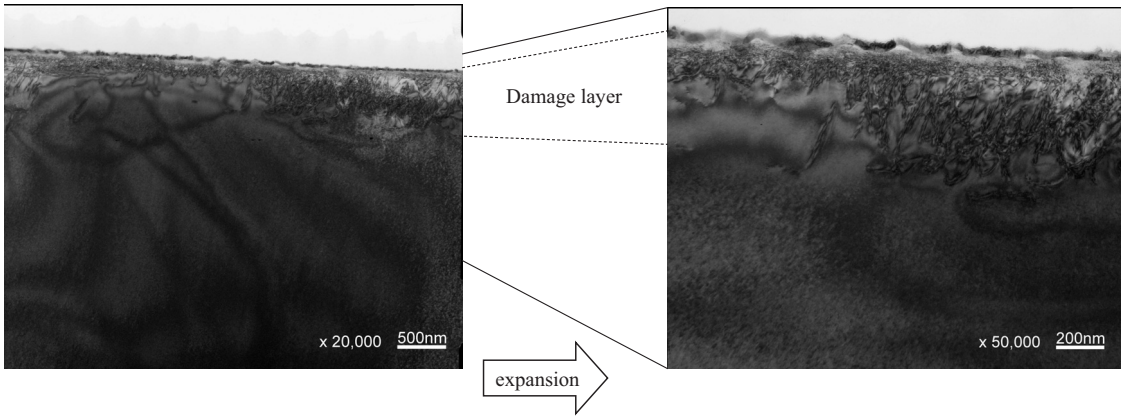

Fig. 8 Cross-sectional transmission electron microscopy (TEM) image of a GaN crystal prepared by flux growth after mechanical polishing

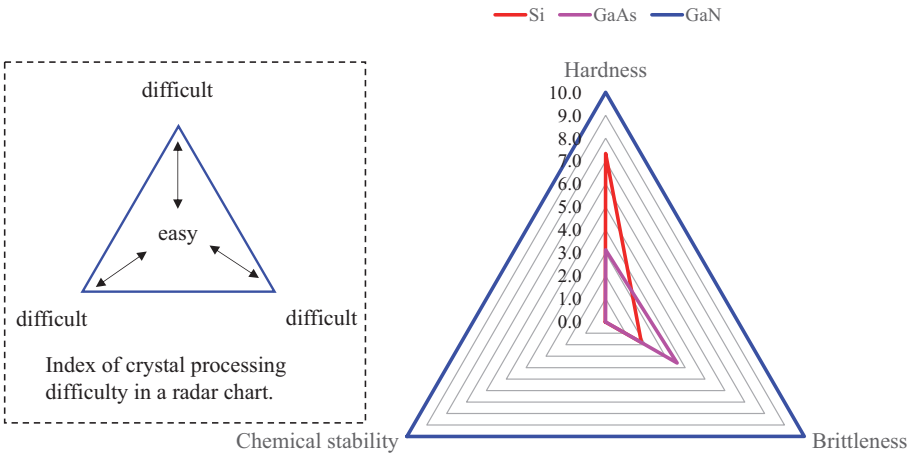

Fig. 9 Radar chart showing GaN vs. Si and GaAs crystals about three key indicators for crystal processing.

the critical depth for the processing mode transition, and the chemical stability is the inverse of the MRR for CMP. Points closer to the origin indicate easier processing, including CMP.

The specific values are as follows. The Vickers hardness values were 1000 several 10 HV for Si, 470 HV for GaAs, and 1000 several hundred–2000 HV for GaN. For the brittleness, increasing the processing load changed the mode from ductile to brittle. The depth at which this transition occurs is known as the critical depth of the processing mode, with a shallower depth resulting in a higher brittleness. The critical depth values were 1 µm for Si, 0.5 µm for GaAs, and just 180 nm for GaN. The MRR values for CMP were several hundred nm/min to several µm/min for Si and GaAs but several nm/min for GaN, which was hundreds to thousands of times slower.

Thus, compared to the other materials, GaN had a high hardness value, resulting in a slower MRR during machining; a high brittleness that promoted the formation of a damaged layer; and high chemical stability, which slowed the CMP-based removal of this damaged layer. These factors also increased the overall processing difficulty.

2. Removal of damaged layers from GaN crystals by CMP

The CMP of GaN crystals involves two main steps.

(1) Oxidizing the GaN surface to form gallium oxide

(2) Removing the gallium oxide using abrasive grains harder than gallium oxide

In step (1), the GaN surface is oxidized with an acidic or a basic slurry to produce gallium oxide. The slurry contains a liquid lubricant and solid abrasive grains, with the lubricant also reducing the friction between the CMP pad (described below), abrasive grains, and crystal material. In step (2), if the hardness values of the materials satisfy the relationship shown below, only gallium oxide is mechanically removed by the abrasive grains, preventing new processing scratches on the GaN crystal.

Gallium oxide < Abrasive grains < GaN

A GaN crystal surface with no damaged layer is obtained by performing CMP with sufficient processing to remove the damaged layer completely.

We used an acidic colloidal silica slurry with an acidic lubricant, optimizing the CMP conditions to produce a GaN crystal surface with no damaged layer. Quartz (SiO_2), which has the same composition as colloidal silica, has a Vickers hardness of greater than 900 HV, making it harder than stoichiometric Ga_2O_3 (650–770 HV) but softer than GaN (1000 several hundred –2000 HV). Common CMP pads include urethane foam, non-woven fabric, and suede. Here, a suede pad was used.

Fig. 10 presents the results. **Fig. 10(a)** shows a CL planar image of the GaN crystal surface before CMP, that is, after the final mechanical polishing. Numerous straight dark lines are visible. The thickness and grayscale values of these lines vary. The field domains between lines appear gray. The amorphous, polycrystalline, mosaic, and cracked layers in the damaged layer described in the previous section exhibit single-crystal disorder, creating non-radiative recombination centers even in direct-bandgap GaN, and producing dark lines, dark areas, and grayscale emission even under electron beam irradiation. These

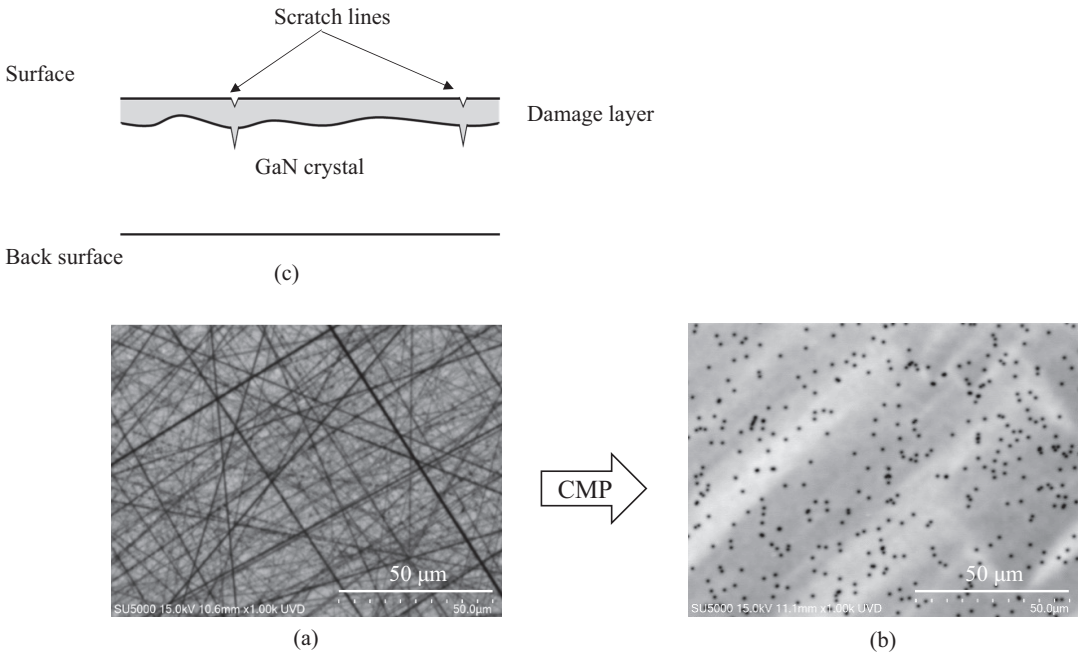

Fig. 10 Plane-view CL image of a GaN crystal (a) before and (b) after CMP, and (c) Cross-sectional schematic of the GaN crystal before CMP.

observations indicate that the damaged layer spanned the surface, with deeper scratches appearing as darker lines and areas. **Fig. 10(c)** shows a cross-sectional schematic. The damaged layer extends several hundred nanometers and exists across the entire surface, with depth variation suggesting deep scratch lines in some areas. The GaN crystal surface with this damaged layer was subjected to the abovementioned CMP process, with **Fig. 10(b)** showing a CL planar image after CMP. The dark lines and areas seen in **Fig. 10(a)** are absent in **Fig. 10(b)**. The dark spots remain in **Fig. 10(b)**, indicating that threading dislocations along the c-axis formed during crystal growth, which are visible as non-radiative recombination centers and appear as threading dislocations on the surface. In other words, after CMP, only dark spots from threading dislocations are observed on the GaN crystal surface, whereas the other field domains are luminescent domains, indicating no planar or linear damaged layer remains. In GaN crystals with direct-bandgap threading dislocations, if a damaged layer is present near the crystal surface, then dark lines and dark areas are observed in CL planar images. This insufficient contrast between the dark spots caused by threading dislocations and the field domains makes the dark spots difficult to observe. Meanwhile, removing this damaged layer restores the contrast between the dark spots caused by threading dislocations and the field domains, clearly revealing the threading dislocations.

Conclusion

Unlike that of other semiconductor crystals, the melt growth of GaN crystals is difficult. This has led to technological advances centered on vapor-phase growth, resulting in multiple technological innovations that have led to the development of current light-emitting devices. In future power-electronic device applications, particularly vertical devices requiring high injection-current densities, the vertical crystal defects caused by crystal growth will need to be reduced. This study demonstrated that IDs, which are one of these defects, can be resolved by combining HVPE with the Na flux method, which is a type of liquid-phase growth method.

Furthermore, because of its physical properties and the characteristics resulting from crystal growth, GaN crystals are more difficult to process than other semiconductor crystals and are prone to developing damaged layers, which are difficult to remove. The presence of a damaged layer necessitates its complete removal to prevent vertical crystal defects and current leakage during epitaxial growth or device fabrication. This study found that CMP, as a final processing step in crystal processing, can yield a GaN crystal surface that is free of damaged layers.

In summary, GaN is challenging to grow and process. However, GaN crystals are required to achieve higher qualities, larger diameters, and lower costs.

Thus, continuous technological innovation is required in both crystal growth and processing methods. We view crystal growth and processing as complementary technologies and aim to meet future societal needs through their continuous development.

References

1) T. Suzuki, *et al.*; The Review of Laser Engineering; 1, 176 (1973).
2) K. Yamaguchi, *et al.*; Journal of the Japan Institute of Metals and Materials; 53, 1140 (1989).
3) W. Utsumi *et al.*, Nature Materials, 2, 735 (2003).
4) J. Karpinski *et al.*, J. Cryst. Growth, 66, 1 (1984).
5) T. Detchprohm *et al.*, Jpn. J. Appl. Phys., 31, L1454 (1992).
6) H. Shin *et al.*, J. Cryst. Growth, 236, 529 (2002).
7) S. Porowski and I. Grzegory, J. Cryst. Growth, 178, 174 (1997).
8) H. Yamane *et al.*, Chem. Mater., 9, 413 (1997).
9) D. R. Ketchum and J. W. Kolis, J. Cryst. Growth, 222, 431 (2001).
10) H. P. Muraska and J. J. Tietjen, Appl. Phys. Lett., 15, 327 (1969).
11) J. I. Pankove *et al.*, RCA Review, 32, 383 (1971).
12) I. Akasaki *et al.*, J. Cryst. Growth, 98, 209 (1989).
13) S. Nakamura, Jpn. J. Appl. Phys, 30, L1705 (1991).
14) H. Amano *et al.*, Jpn. J. Appl. Phys, 28, L2112 (1989).
15) S. Nakamura *et al.*, Jpn. J. Appl. Phys, 30, L1708 (1991).
16) K. Motoki *et al.*, Jpn. J. Appl. Phys, 40, L140 (2001).
17) Y. Ohshima *et al.*, Jpn. J. Appl. Phys, 42, L1 (2003).
18) K. Fujito *et al.*, J. Cryst. Growth, 311, 3011 (2009).
19) H. Fujikura, *et al.*; SUMITOMO KAGAKU, 2018, 38 (2018).
20) M. Tajima, *et al.*; “Shirikon Kessho Gijutsu -Seicho, Kako, Kekkan Seigyo, Hyoka-“ [Silicon Crystal Technology -Growth, Processing, Defect Control, and Evaluation-]; Japan Society for the Promotion of Science Committee 145 Technology Succession Project Editorial Committee (2015), p. 148.
21) S. Sarayama, *et al.*; “Jisedai Handotai-yo no Nankako Kessho Zairyo no tame no Choseimitsu Kako Gijutsu” [Ultraprecision Machining Technology for Hard-to-Machine Crystal Materials for Next-generation Semiconductors]; R&D Support Center (2024), p. 97.
22) M. Matsunaga, *et al.*; “Erekutoronikusu-yo Kessho Zairyo no Seimitsu Kako Gijutsu” [Precision Machining Technology for Crystal Materials for Electronics]; Science Forum (1985), p. 579.

PROFILE

Seiji Sarayama

Sumitomo Chemical Co., Ltd.
ICT & Mobility Solutions Research Laboratory

Takashi Sato

Sumitomo Chemical Co., Ltd.
ICT & Mobility Solutions Research Laboratory
Manager